REPORT DOCUMENTATION PAGE

Form Approved OMB No. 0704-0188

1. REPORT DATE *(DD-MM-YYYY)*	2. REPORT TYPE	3. DATES COVERED *(From – To)*
09-04-2010	Final Report	01-Feb-08 - 19-Jul-10

4. TITLE AND SUBTITLE

Annular Electric Discharge as a Combustion Igniter in a Supersonic Flow

5a. CONTRACT NUMBER
ISTC Registration No: 3833P

5b. GRANT NUMBER

5c. PROGRAM ELEMENT NUMBER

6. AUTHOR(S)

Kossyi Igor Antonovich

5d. PROJECT NUMBER

5d. TASK NUMBER

5e. WORK UNIT NUMBER

7. PERFORMING ORGANIZATION NAME(S) AND ADDRESS(ES)
A.M.Prokhorov General Physics Institute of Russian Academy of Sciences
Vavilov Street 38
Moscow 119991
Russia

8. PERFORMING ORGANIZATION REPORT NUMBER

N/A

9. SPONSORING/MONITORING AGENCY NAME(S) AND ADDRESS(ES)

EOARD
Unit 4515 BOX 14
APO AE 09421

10. SPONSOR/MONITOR'S ACRONYM(S)

11. SPONSOR/MONITOR'S REPORT NUMBER(S)
ISTC 07-7012

12. DISTRIBUTION/AVAILABILITY STATEMENT

Approved for public release; distribution is unlimited.

13. SUPPLEMENTARY NOTES

14. ABSTRACT

This report results from a contract tasking A.M.Prokhorov General Physics Institute of Russian Academy of Sciences as follows: The main object of this Project is investigation of combustion processes in a gas mixtures flows under the action of axially symmetric gas discharge localized on the periphery of gas stream. Complexity and peculiarity of this discharge action on a flammable gases flow consists in excitation on a periphery combustion wave with concurrent generation of convergent to the axis cumulative shock wave transforming near the axis into a detonation one. Of interest is research of gas stream volumetric ignition at the sacrifice of action on it periphery plasma and focusing in a near-axis region shock wave.
Experiments in the moving gas and gas in the quiescent state as well as development of mathematical model of investigating phenomenon are planning.

15. SUBJECT TERMS
EOARD, Propulsion, Engines And Fuels, Combustion and Ignition

16. SECURITY CLASSIFICATION OF:			17. LIMITATION OF ABSTRACT	18, NUMBER OF PAGES	19a. NAME OF RESPONSIBLE PERSON
a. REPORT	b. ABSTRACT	c. THIS PAGE			Stephanie Masoni, Maj, USAF
UNCLAS	UNCLAS	UNCLAS	UL		19b. TELEPHONE NUMBER *(Include area code)* +44 (0)1895 616420

ISTC PROJECT NO. 3833P

ANNULAR ELECTRIC DISCHARGE AS AN INITIATOR OF COMBUSTION IN SUPERSONIC FLOW

FINAL PROJECT TECHNICAL REPORT

ON THE WORK PERFORMED FROM FEBRUARY 1, 2008 TO FEBRUARY 1, 2010

A.M. Prokhorov General Physics Institute, Russian Academy of Sciences

Project Manager	**I.A. Kossyi** **Dr. Sci. (Phys.&Math.)**	
Director	**I.A. Shcherbakov** **Corresponding Member of the RAS**	

February 2009

This work is supported financially by EOARD and performed under the agreement with the International Science and Technology Center (ISTC), Moscow.

Title of the Project:	Annular electric discharge as an initiator of combustion in supersonic flow
Contracting Institute:	A.M. Prokhorov General Physics Institute, Russian Academy of Sciences
Commencement Date:	February 1, 2008
Duration:	24 months
Project Manager	Kossyi Igor Antonovich
phone number:	+7 499 135-41-65
fax number:	+7 499 135-80-11
e-mail address:	kossyi@fpl.gpi.ru
Leading Institution:	A. M. Prokhorov General Physics Institute of the Russian Academy of Sciences, 119991, Vavilov Street 38, Moscow Russia Phone number: (499) 135-13-30 Email: mineev@kapella.gpi.ru
Participating Institutions:	
Foreign Collaborators:	European Office of Aerospace Research and Development (EOARD)

Keywords:
gliding surface discharge, toroidal shock wave, Mach shock waves, cumulation of non-one-dimensional shock waves, gas temperature on shock wave focus, methane--oxygen mixture, combustion

CONTENTS

Brief description of the work plan: objective, expected results, technical approach

The prime objective of the project is to investigate combustion processes in gas mixture flows under the action of axisymmetric discharges produced at the periphery of these gas flows. The complexity and peculiarity of the action of these discharges on combustible gas flows is that the excitation of a combustion wave at the periphery would be accompanied by generation of a cumulative shock wave converging toward the axis and being able to transform into a detonation wave near the axis.

It is therefore important to study the initiation of volume combustion in the gas flow due to the plasma action at the periphery and due to focusing of a shock wave in the axial region.

We planned to carry out experiments in chemically inactive and combustible gas mixtures and to develop mathematical models of the phenomena under study.

One scheme we have suggested for realizing the action of an annular discharge on a combustible gas flow is shown in Fig. 1. Here, the annular discharger is placed at the periphery of the gas flow in a tube. Such a discharger is made up of rings located on the surface of a circular dielectric base. A pulsed voltage applied to the rings produces local gliding surface discharges. This annular plasma initiates a combustion wave, which is propagated through the surrounding gas. This combustion wave is left behind a cumulative converging shock wave formed by the discharger.

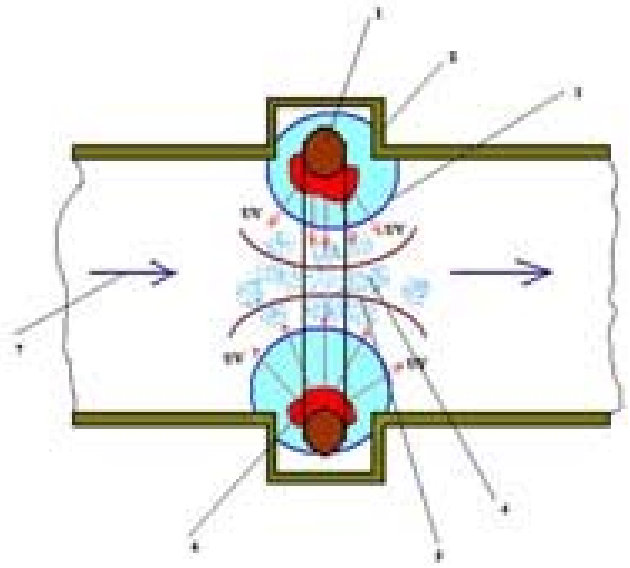

Fig. 1.
Schematic diagram of the action of annular gliding surface discharge on a combustible gas stream: (1) annular discharger, (2) combustion chamber, (3) peripheral combustion wave, (4) gas activated by UV and IR radiation, (5) cumulative shock wave, (6) annular gliding surface discharge plasma, and (7) combustible gas stream.

A high temperature attainable at the front of the converging shock wave can initiate combustion of the gas mixture near the axis, which may be considered as a factor with a beneficial effect on combustion initiation throughout the entire gas volume.

The cumulative effect of a converging toroidal shock wave was demonstrated for the first time in experiments carried out at the GPI, with a shock wave in air. Analysis of the processes of convergence and reflection of non-one-dimensional shock waves has been performed by I.V.

Sokolov, who based on analytical approach to the problem, developed a theory of cumulative processes in toroidal shock waves.

Experiments carried out at the GPI have first shown that the one-dimensional or non-one-dimensional geometry in itself is of little consequence for the cumulative process of shock waves. A shock wave produced and investigated in the experiment was ring-shaped (toroidal), apparently non-one-dimensional. It was shown that the intensity of the shock wave generated by an annular electric-discharge source begins to grow when approaching the center of the ring. Generally, the cumulative process of a non-cylindrical (non-spherical) shock wave arriving at the axis is not a trivial fact, because in contrast to one-dimensional waves, in the non-one-dimensional case there hydrodynamic energy outflow in the direction along the axis.

Theoretical analysis performed by I.V. Sokolov has shown that, if dissipative processes are ignored, the amplitude of a ring shock wave (as well as spherical and cylindrical waves) increases without bound.

It should be noted that one of the peculiarities of the cumulative process of collapse of a torodal shock wave is the irregular behavior (Mach shock wave) at reflections at the symmetry axis at small values of the axial coordinate, where the radial motion transforms to the axial motion.

The unbounded energy increase of the convergent shock wave is indicative of a cumulative process but presents the main problem unresolved in both theory and experiment - that is, an understanding of mechanisms that in a real situation set limits to energy values on the focus.

According to the self-similar solution obtained for a spherical shock wave, the gas density on the focus (ρ_f) is finite ($\rho_f \cong 21.6\ \rho_0$). The conclusion that there is a finite density in the focal region is apparently applicable to three-dimensional shock waves. This result indicates an unbounded increase in the gas temperature T_g behind the wave front. The present-day theory fails to offer mechanisms of dissipation of the wave energy that would limit the increase in T_g as a shock wave approaches its focus, while there are practically no experimental data on the gas temperature T_g in the vicinity of the focus.

The objective of the Project was to carry out experiments and numerical simulations in order to estimate the possibility of local gas heating a in the focal region of a convergent shock wave. The study was stimulated, in particular, by the applied problem central to the Project, namely, the initiation of combustion of air--fuel streams in the axial region of the combustion chamber.

The proposed study pertains to fundamental physics.

We planned to accomplish the following tasks in the course of implementation of the present Project.

Task 1. To design, manufacture, and put into operation an experimental setup for studying the process of focusing non-one-dimensional (toroidal) shock waves generated by annular electric discharge in quiescent air at atmospheric pressure. To prepare a diagnostic system for measuring the dynamics of shock waves and the gas parameters;
Task 2. To develop a mathematical model of the cumulative effect of a non-one-dimensional shock wave in a chemically inactive gas;
Task 3. To determine (or estimate) a value of the gas temperature attainable in the focal region of the toroidal wave excited in air at atmospheric pressure, on the basis of the above experiments and calculations;
Task 4. To design, manufacture, and put into operation an experimental setup for studying the process of focusing non-one-dimensional (toroidal) shock waves generated by annular electric discharge in stationary stoichiometric CH_4:O_2 mixtures;
Task 5. To develop a mathematical model of the cumulative affect of a toroidal shock wave in a methane--oxygen gas mixture;

Task 6. To design, manufacture, and put into operation an experimental setup for studying the process of focusing non-one-dimensional (toroidal) shock waves generated by annular electric discharge in the stoichiometric CH_4:O_2 mixtures;
Task 7. To carry out experiments on distant gas heating and ignition in the streams of stoichiometric CH_4:O_2 mixtures by convergent toroidal shock waves generated by annular electric discharge.

2. Results

Main results obtained in the course of execution of first three tasks (Task 1, Task 2, Task 3) are the following:

To accomplish the experimental program of the Project, we have assembled the experimental setup in which the basic unit was an annular multielectrode discharge system. A high-current discharge was excited along the inner surface (which faced the Z-axis) to form an annular plasma layer that gave rise to a toroidal (ring) shock wave converging toward the axis.

Figure 2 shows a photograph of the electric discharger ready for mounting at the bench and also a photograph of the discharger during operation after applying a high-voltage pulse exciting a gliding surface discharge. The electric circuit generating high-voltage pulses is shown in Fig. 3. After triggering switch P, capacitor C, which is charged to voltage U, begins to discharge through ring discharger (1). The diameter of the annular discharger is $D_d \cong 10$ cm. The ring thickness is $2h \cong 1.2$ cm. The energy released in each discharge pulse is $E_0 \leq 200$ J. The discharge is excited in air at atmospheric pressure.

(a)

(b)

Fig. 2.
Photograph of the electric discharger generating a continuous annular plasma layer:
(a) before mounting at the experimental bench, and

(b) in operating condition during high-voltage pulse

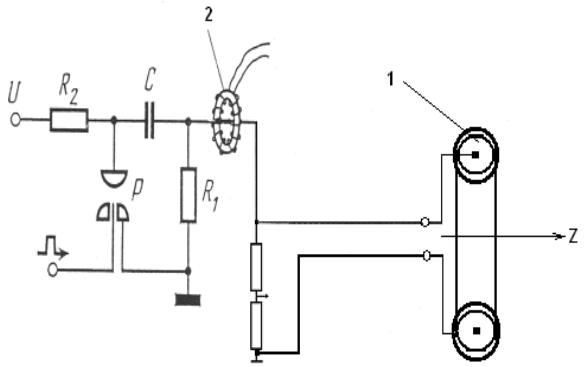

Fig. 3.
Electric circuit for exciting the annular discharger:
(1) annular discharger; (2) Rogowski coil.

Measurements of the dynamics of the toroidal shock wave were based at several diagnostics:

- Shadow photography, which makes it possible to trace the dynamics of the formation and radial convergence of the shock wave;
- Measurements of excess pressure at different points at the Z- axis, which passes through the center of the annular discharger, and also at different positions of the pressure sensor in the radial direction. As a gauge, we used a pressure sensor (PCB PIEZOTRONICS model 132A32), which allows measurements of the excess pressure $\Delta p \leq 3.5$ atm with a time resolution about 0.5 μs;
- Method of laser "refraction" detector, used to detect the axial (Mach) shock wave and the radial motion gas-dynamic perturbations excited by annular discharge.

Typical successive shadow pictures are shown in Fig. 4. In each realization, we took four photographs with exposure $t_{exp} \approx 2$ μs and delays between frames of ≈ 2 μs. Four successive frames for each realization are arranged in the following order: from left to right, from top to bottom. The delay time Δt, counted from the switching-on of the high-voltage pulse, was varied from one realization to another.

In the photographs, we observe a well-defined toroidal (ring) shock wave that converges at the axis of the ring (Figs. 4a-4d). The time interval between the discharge initiation and the shock wave focusing (frame no.16 in Fig. 4d) is $\Delta t_f \approx 77$ μs.

The shock wave reflected at the axis is observed in Fig. 4e. To illustrate details, Fig. 5 shows the enlarged frames of Fig. 4e. A distinct perturbation observed near the axis in Fig. 4e (frame nos. 19, 20) and also in Fig. 5 may be attributed to the gas heating in the focal region.

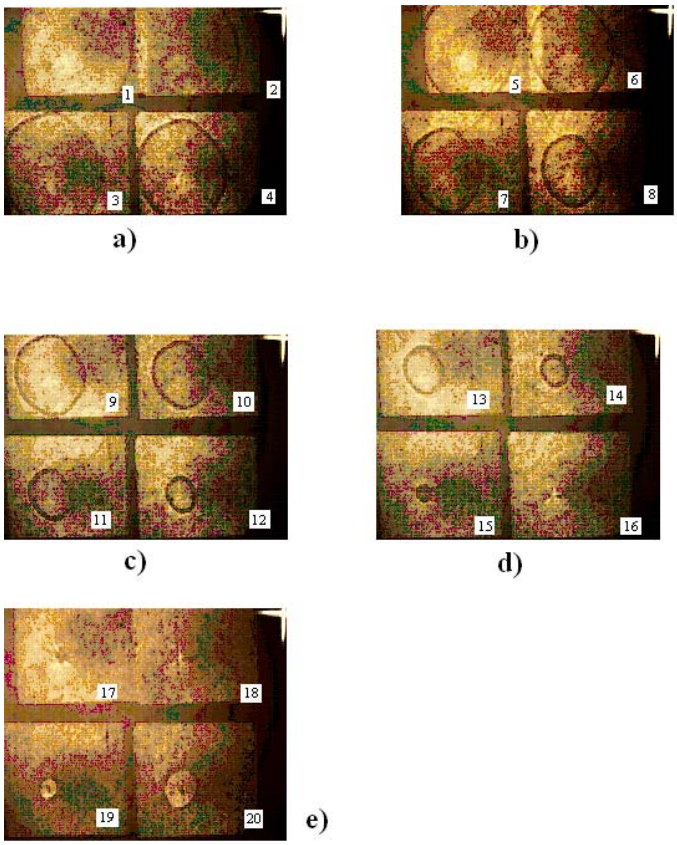

Fig. 4.
Typical successive shadow photographs taken with the help of the KADR IOFAN streak camera with different delay times Δt, counted from the switching-on of the high-voltage pulse: (a) Δt_1 = 13 μs, (b) Δt_2 = 25 μs, (c) Δt_3 = 45 μs, (d) Δt_4 = 65 μs, and (e) Δt_5 = 85 μs. The field of view is 2x2 cm.

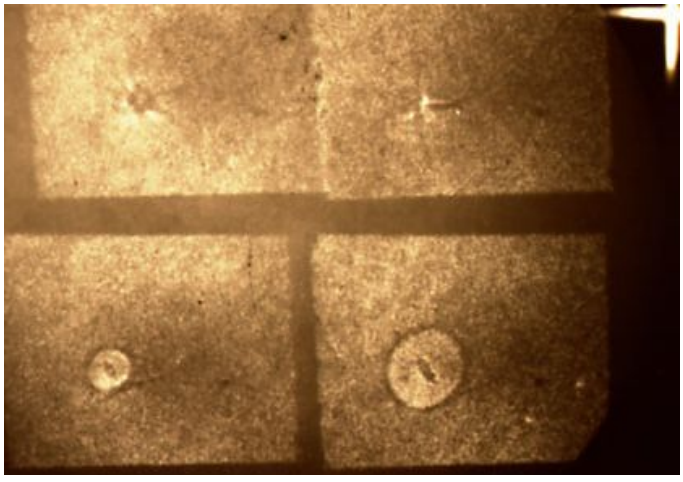

Fig. 5.
Enlarged frame of Fig. 4e for illustration of details of the shadow picture of the region of focusing of the toroidal shock wave; Δt_5 = 85 μs.

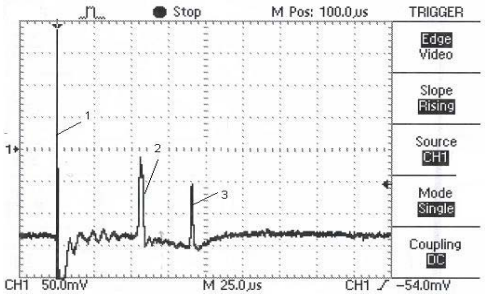

a)

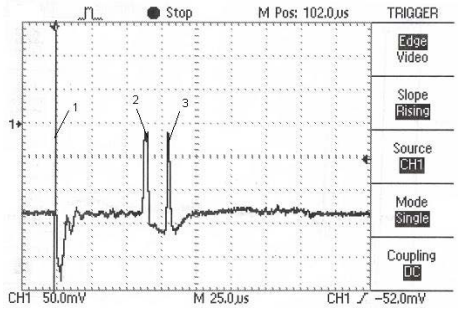

b)

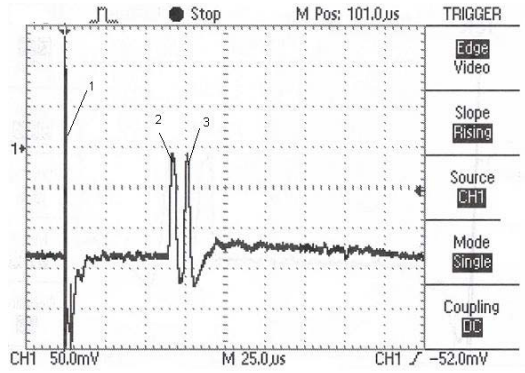

c)

Fig. 6.
Typical oscillograms of signals from the refraction detector. Diagnostic laser beam is orthogonal to the plane of the annular discharger.

Figure 6 shows typical oscillograms obtained at the radial displacement (Δr) of the diagnostic beam of the refraction detector. In the figures, signal (1) corresponds to pickup in the detector circuit when a high-voltage pulse is applied to the annular discharger. Signal (2) has been associated with the refraction of the diagnostic laser beam at the front of the toroidal shock wave convergent at the axis, and signal (3) has been associated with the refraction at the shock wave reflected from the ring axis. As the diagnostic laser beam is displaced from the discharger toward the axis, signals (2) and (3) become closer and closer to one another, merging in the focal (axial) region. The instant of merging correspond ro the delay time of the focusing of the shock wave with respect to the triggering of the discharge. This delay time is $\Delta t_f \cong 76$ μs, which is close to that obtained by analyzing shadow photographs.

Axial propagation of gas-dynamic perturbations accompanying the focusing of the toroidal wave was studied with the help of the pressure sensor by displacing it along the Z-axis from shot to shot , as well as with refraction measurements in which the diagnostic laser beams were separated a distance ΔZ along the Z-axis over . A typical signal of the pressure sensor is shown in Fig. 7. Here, signal (1) corresponds to pickup in the sensor circuit when a high-voltage pulse is applied to the annular discharger. Signal (2) is caused by gas-dynamic perturbation (shock

wave) arrived at the sensor front surface. Signal (3) is a spurious signal caused by internal reflection of the acoustic wave from the sensor components.

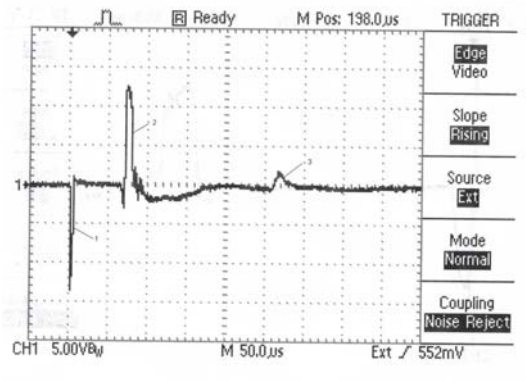

Fig. 7.
Typical oscillogram of the signal from the pressure sensor.
$\Delta z \cong 1$ cm.
Signal (1) is due to pickup in the sensor circuit when a high-voltage pulse is applied to the annular discharger, signal (2) is due to the Mach (axial) shock wave, and signal (3) is a spurious signal.

Figure 8 illustrates a typical signal from the refraction detector displaced along the Z-axis. Signal (1) is caused by the refraction of the diagnostic laser beams intersecting at the convergent toroidal shock wave before the focusing and a double signal (2) is caused by the refraction of the laser beams by the axially propagating shock wave accompanying the focusing of the toroidal shock wave.

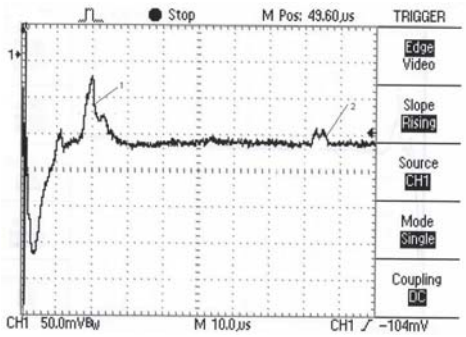

Fig. 8.
Typical oscillogram of the signal from the refraction detector.
Diagnostic laser beams are orthogonal to the Z-axis.
$\Delta z \cong 0.9$ cm
Signal (1) is caused by refraction of the laser beam by peripheral gas-dynamic perturbations; signal (2) is caused by refraction by the Mach (axial) shock wave.

The results of measuring the z-coordinate of the front of gas-dynamic perturbation are presented in Fig. 9.

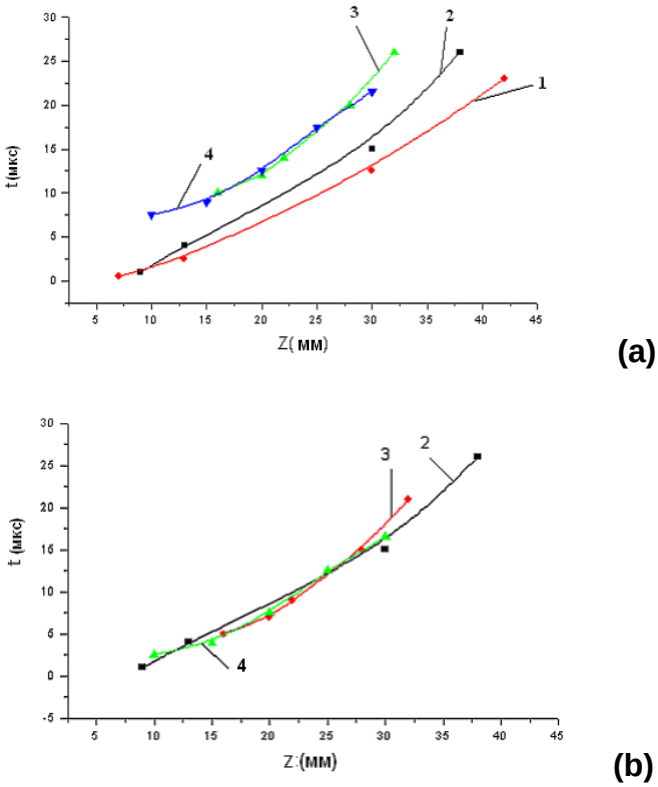

Fig. 9.
Time dependence of the z-coordinate (r = 0) of the front of the Mach (axial) shock wave:
(1) calculated curve for E_0 = 500 J,
(2) calculated curve for E_0 = 200 J,
(3) experimental curve (measurements with the refraction detector),
(4) experimental curve (measurements with the pressure sensor).

We numerically solved the problem of a gas flow initiated by instantaneous energy release from a toroidal electric discharge in quiescent air (21% O_2, 78% N_2, 1% Ar) at normal conditions (p_0 = 1 atm, T_{g0} = 298 K). In our model, this energy release was accounted for by a corresponding increase in the internal energy of the gas mixture in a specified discharge region.

The set of equations describing axisymmetric two-dimensional non-steady-state nonviscous gas flows is as follows:

$$\frac{\partial(r\rho)}{\partial t}+\frac{\partial(r u\rho)}{\partial z}+\frac{\partial(rv\rho)}{\partial r}=0 \qquad (1)$$

$$\frac{\partial(r\rho u)}{\partial t}+\frac{\partial\left(r\left(\rho u^2\right)+p\right)}{\partial z}+\frac{\partial(r\rho uv)}{\partial r}=0 \qquad (2)$$

$$\frac{\partial(r\rho v)}{\partial t}+\frac{\partial(r\rho vu)}{\partial z}+\frac{\partial\left(r\left(\rho v^2+p\right)\right)}{\partial r}=0 \qquad (3)$$

$$\frac{\partial\left(r\left(\rho\left(u^2+v^2\right)/2+\rho h-p\right)\right)}{\partial t}+\frac{\partial\left(ru\left(\rho\left(u^2+v^2\right)/2+\rho h\right)\right)}{\partial z}+\frac{\partial\left(rv\left(\rho\left(u^2+v^2\right)/2+\rho h\right)\right)}{\partial r}=0, \qquad (4)$$

where z and r are the longitudinal and radial coordinated, respectively; u and v are the corresponding velocity components; t is the time ; ρ, p and h are the mass density, pressure and enthalpy of the gas, respectively.

The multicomponent gas mixture was described using the following equations of state of an ideal gas:

$$p = \rho R_0 T_g \Sigma n_i,\ h = \Sigma n_i h_i(T_g), \quad i = 1,2,3, \qquad (5)$$

where T_g is the gas temperature; R_0 is the absolute gas constant; and n_i are the concentrations of the gas-mixture components were assumed to be constant and equal to their initial values. The temperature dependences of the partial enthalpies $h_i(T_g)$ were derived by approximating the tabulated data.

With the initial data mentioned above, the flow was symmetric about the equatorial plane of the toroidal discharge region.

The gas-dynamic equations were solved numerically in finite differences by using the scheme proposed by S.K. Godunov; a two-dimensional stationary grid was generated without separating discontinuity surfaces. As the axis of symmetry $r = 0$ was approached, the mesh size in the radial direction was gradually reduced because of the presence of converging streams in the flow. The mesh size was selected so as to minimize the computation time and, at the same time, to ensure a reasonable accuracy of solution. Thus, the radial mesh size Δ_r for $r \in (0, R_0 - r_0)$ varied from 0.017 mm (near the axis of symmetry) to 0.197 mm (near the region of energy release), Δ_r = 0.167 mm was taken for $r \in (R_0 - r_0,\ R_0 + r_0)$, and for $r \in (R_0 + r_0,\ 4R_0)$ Δ_r varied from 0.167 mm to 0.34 mm. The longitudinal mesh size was Δ_z = 0.2 mm.

The calculations were performed for toroidal discharges with R_0 = 0.05 m and released energy E_0 = 200 and 500 J.

Figures 10 and 11 show the pressure distributions at r = 0 calculated for the stage subsequent to focusing of the toroidal wave generated at released energies E_0 = 200 J and E_0 = 500 J, respectively.

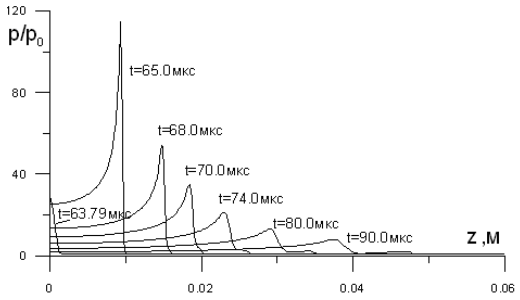

Fig. 10.
Calculated pressure dependences on the longitudinal coordinate z (r = 0)
at various times. E_0 = 200 J.

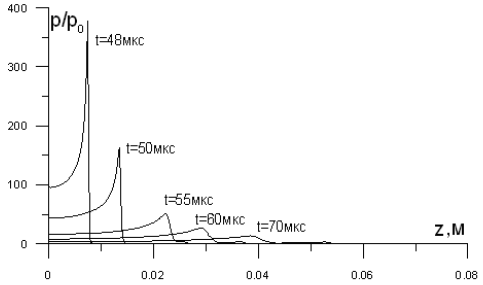

Fig. 11.
Calculated pressure dependences on the longitudinal coordinate z (r = 0)
at various times. E_0 = 500 J.

The dependences of the wavefront coordinates of the axially propagating shock waves z_{fr}, determined from Figs. 10 and 11 are presented in Fig. 9a, where the calculated curves are compared with experimental ones.

Figure 12 shows the calculated peak values of the gas temperature T_g attained at the front of the axially propagating shock waves at different points at the Z-axis in the region close to z = 0 (to the focus of the toroidal shock wave).

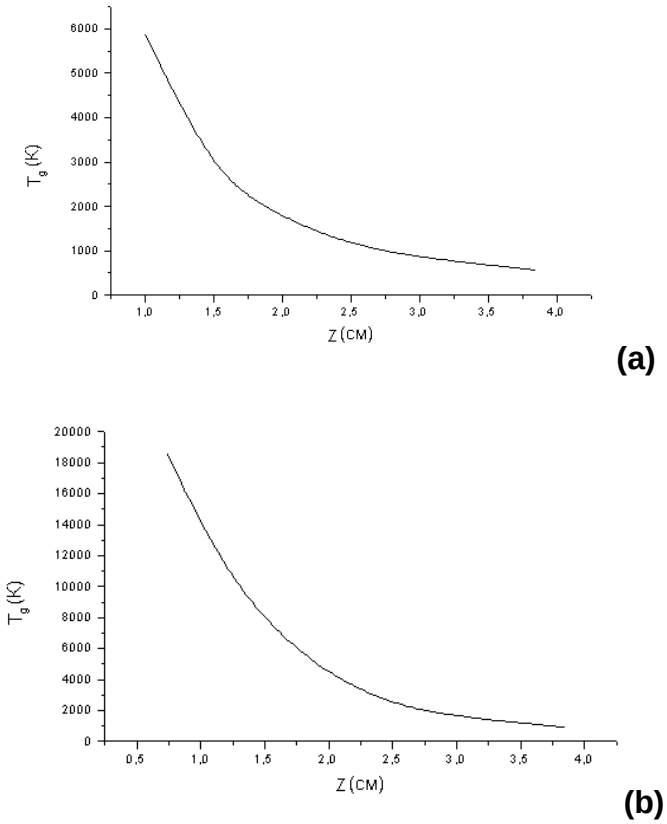

Fig. 12.
Peak values of temperature T_g attainable at the front of the Mach wave
at different points at the Z-axis;
(a) calculations with E_0 = 200 J, (b) calculations with E_0 = 500 J.

Comparison of the measured and calculated coordinates in Fig. 9 shows that the measured time dependence correlates with calculations assuming that the energy released in the annular discharger is E_0 = 200 J. The experimental points, however, lie somewhat above the calculated curve. Such a discrepancy may be attributed to the assumption of instantaneous energy release adopted in our simulations. If we take into account that the duration of energy release in the annular discharger in our experiment is ~5 μs, then, introducing a correction for this time interval, we achieve closer agreement between the measured and calculated dependences $\tau_f(z)$.

Satisfactory agreement in Fig. 9a allows us to conclude that theory adequately describes cumulative convergence of a torodal shock wave under study, in particular, the axial propagation of a Mach shock wave formed due to irregular reflections of a non-one-dimensional shock wave at the symmetry axis. This indicates that the gas temperature at the axis corresponds to calculations assuming E_0 = 200 J and, according to Fig. 11a, the gas temperature reaches $T_g \cong 6000$ K at a distance $z \cong 1$ cm from the center of the annular

discharger and drops to $T_g \cong 1000$ K at a distance $z \cong 3$ cm. Note that, here we speak about the peak value of gas temperature that is reached when the front of a Mach shock wave (axial shock wave) arrives at this coordinate z_f. For the interval $1 \leq z_f \leq 2$ cm, the temperature remains high enough ($T_g \geq T_{gm}/2$, where T_{gm} is the temperature behind the front of the axially propagating shock wave) during the time from a fraction of a microsecond to several microseconds.

The values of T_{gm} increase considerably with increasing E_0 to 500 J (see Fig. 12b). It should be remembered, however, that dissipative processes were ignored in the calculations. The actual temperatures near z = 0 may thus be lower than predicted in Fig. 12b, according to which the temperature at $z_f \cong 1$ cm attains values on the order of $T_g \approx 18000$ K.

The shadow photographs (Fig. 5) with a characteristic dark spot, which demonstrate that the toroidal shock wave does converge after its reflection at the axis, show evidence of the gas heating in the axial region of the annular discharge. However, the photographs give no way of evaluating the gas temperature.

Thus, it follows from the experiments and calculations that, at energy release per unit length $\varepsilon_0 \geq 5 - 10$ J/cm, it is possible to heat the gas up to temperatures above several thousands of Kelvins in a small volume $V_f < 10^{-3}$ cm^3, in the axial region located some distance away from the discharger . The energy transfer from the discharge to this region occurs through gas-dynamic perturbations generated by the discharge.

Both the above experiments and calculations, being of fundamental importance themselves, were stimulated, however, by the applied problem - initiation of combustion of fuel-air streams in the axial region of a ramjet aviation engine. Considering the obtained results from this viewpoint, we should mention that the heating of a gas to the ignition temperature of the mixture would realized in relatively small volumes, and the temperature would maintained at a high level for a short (microsecond) time. Now, we are not in position to assert that the ignition of a air-fuel stream is realizable. However, this possibility cannot be excluded, first of all, in connection with a series of experiments on initiation of combustion of gas mixtures by laser sparks, microwave discharges and gliding surface discharges, which have revealed the generation of long-lived high-temperature microscopic plasma objects eventually causing volume combustion of gas mixtures.

Experimental studies of the processes accompanying the excitation of ring discharge in a stoichiometric methane—oxygen mixture in closed chamber, were carried out according to the tasks of the Work plan listed in the previous section: Task 4, Task 6 and Task 7.

To study the action of a ring electric discharge on a chemically active (combustible) gas, we designed, assembled and put into operation an experimental setup shown schematically in Fig. 13. A cylindrical organic-glass reactor chamber is 100 mm in diameter and 70 mm in height. Its ends are covered with plane-parallel quartz windows. The chamber is evacuated to a pressure $p_0 < 0.1$ Torr and filled with a stoichiometric mixture CH_4:O_2 = 60:120 Torr or oxygen (to a pressure $p \cong 180$ Torr).

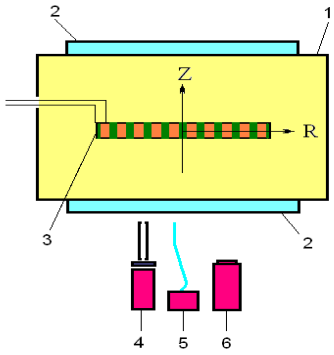

Fig. 13.
Schematic of the experiment: (1)-vacuum chamber, (2) quartz windows, (3) annular discharger, (4) collimated photomultiplier, (5) spectrograph, (6) image converter camera.

As an electric-discharge initiator of combustion of a gas mixture, we used an annular multielectrode system placed inside the chamber. This discharger is a system of insulated ring electrodes (titanium, stainless steel) around a high-voltage metal return conductor. The energy released in discharge during one pulse was ≈40 J. The volume of electric-discharge plasma produced by energy release is ≈ 2 cm^3.

To study a glow accompanying the discharge processes and the combustion of the gas mixture, we used an FEU-39 collimated photomultiplier with a spatial resolution of ≈ 8 mm at the chamber axis. For the same purposes, we used an FER-7 optical streak camera. The radiation of the band of OH radicals was selected from the spectrum with the help of ZhS-20 and UFS-5 filters placed in front of the photomultiplier. In the absence of filters, the photomultiplier signal showed the time behavior of the radiation integrated over the spectrum.

Spectral characteristics of the radiation emitted from the discharge region and the combustion zone were studied with the help of AvaSpec-3648FT spectrograph, which allowed measurements of the spectrum in the wavelength range λ = 200 - 800 nm with a time resolution of up to 10 μs.

Gas-dynamic perturbations of the medium were recorded using shadow photography according to the scheme presented in Fig. 14. A system of lenses (3), (4), incorporated in a telescope, forms a paraxial beam of a pulsed nitrogen laser (λ = 337.1 nm), which passes perpendicular to the cross section of the ring discharger excited by high-voltage pulses of a power supply. The laser beam passed through the cross-sectional area of the discharger is recorded with the help of photographic camera (10). We made successive photographs by varying the delay time of the laser pulse with respect to trigger pulse of the discharger (τ_d). In this way, we traced the time variation of the shadow pattern formed by gas-dynamic perturbations in the plane of the ring, in particular, by toroidal shock wave propagating from the discharger.

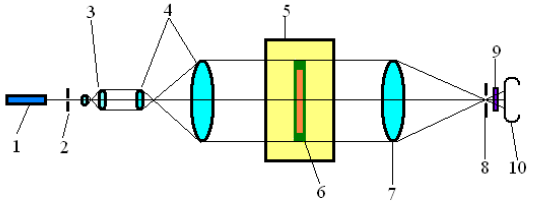

Fig. 14.

Scheme of shadow photography: (1) nitrogen laser; (2, 8) apertures; (3) objective for preliminary expansion of the laser beam; (4) telescope; (5) vacuum chamber, (6) ring discharger; (7) collecting lens; (9) filter; (10) photographic camera.

Figure 15 shows the 'refraction' detector scheme which allows local gas-dynamic perturbations in the plane of a ring discharge to be detected with a high temporal and spatial resolution. A paraxial narrow (~ 1 mm in diameter) beam of helium-neon laser (4) passes through the plane of a ring discharge and falls within the aperture of a diaphragm (6) placed in front of photomultiplier (5). The photomultiplier signal is fed into an oscillograph. The refraction of the laser beam by gas-dynamic perturbations of the medium deflects the beam from the aperture axis and, as a result, the photomultiplier signal decays.

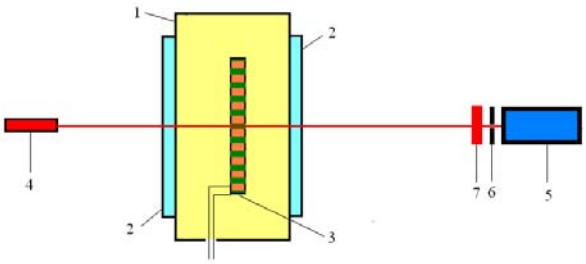

Fig. 15.
Scheme of refraction measurements: (1) vacuum chamber; (2) quartz windows; (3) ring electric discharger; (4) helium-neon laser; (5) photomultiplier FEU-60; (6) diaphragm; (7) interference filter.

Figures 16 and 17 show typical photomultiplier signals corresponding to the intensity of radiation integrated over the spectrum and the OH band radiation of the, respectively, which are observed in the plane of the ring at different distances from the axis (the working gas is a methane—oxygen mixture). Figures 18 and 19 show typical photomultiplier signals corresponding to the intensity of radiation integrated over the spectrum and the OH band radiation, which are observed at different values of the energy released in the ring discharge (the working gas is a methane—oxygen mixture). The radiation is received from the central region of the ring. The curves are normalized to maximal values of radiation intensity in the initiated flame.

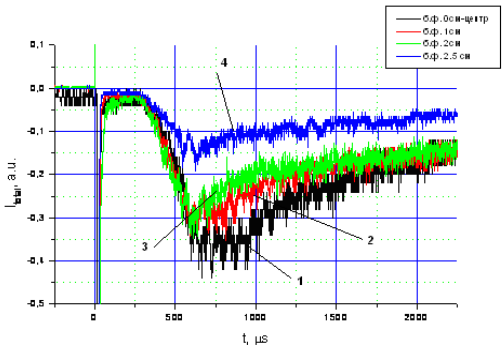

Fig. 16.
Photomultiplier signals corresponding to the intensity of radiation integrated over the spectrum, which are measured at different distances from the center of the ring:

(1) R=0; (2) R=1cm; (3) R=2cm; (4) R=2.5 cm.

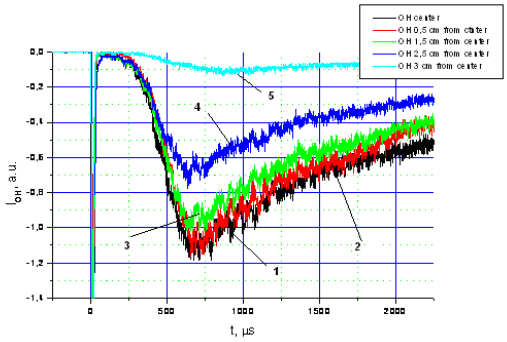

Fig. 17
Photomultiplier signals corresponding to the OH band intensity measured at different distances from the center of the ring:
(1) R=0; (2) R=0.5cm; (3) R=1.5cm; (4) R=3.0 cm.

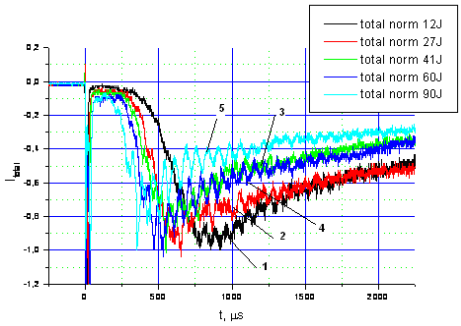

Fig. 18
Photomultiplier signals corresponding to the intensity of radiation integrated over the spectrum, which are measured at different values of energy W released in the ring discharge:
(1) W=12J; (2) W=27J; (3) W=41J; (4) W=60J; (5) W=90J.

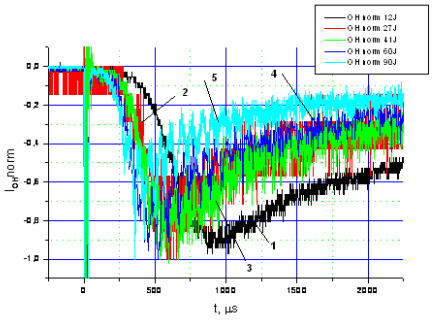

Fig. 19
Photomultiplier signals corresponding to the OH band intensity measured at different values of energy W released in the ring discharge:
(1) W=12J; (2) W=27J; (3) W=41J; (4) W=60J; (5) W=90J.

Figures 20 and 21 show typical photographs of FER-7 streak, taken when its slit is oriented in the radial direction and along the axis Z of the ring, respectively. The temporal and spatial scales are indicated in the figures.

Figure 22 shows typical spectra of the radiation from the reactor, which are obtained with the help of the AVASPEC-3648 spectrograph with an exposure time of 200 μs. The delay time with respect to the discharger trigger pulse is indicated in the figure. At a delay time of 100 μs, the spectrum exhibits the lines λ = 510.55 nm (copper) and λ = 589 nm (sodium). At delay times in the interval 300—600 μs, the band corresponding to the OH radical appears in the spectrum. At delay times of about 500 μ and more, brightness of the OH band reaches its maximum, and a continuum appears in the spectral region 450—600 nm, in which the bands of C_2, CO, CO_2 molecules are also present.

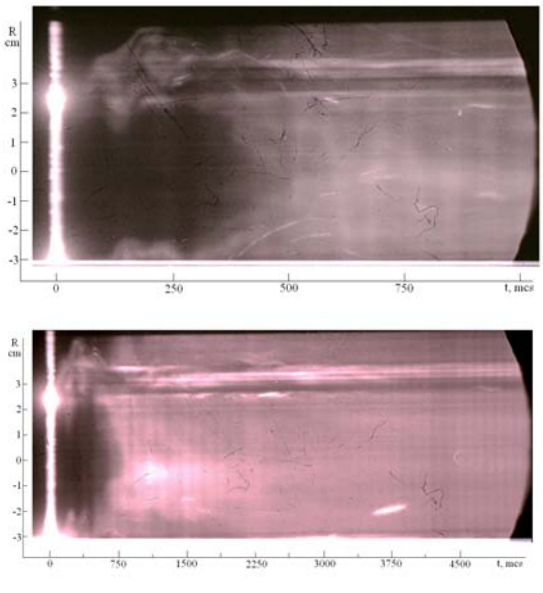

(a)

(b)

Fig. 20

Typical streak images of glow in the reactor. The slit of the streak camera is oriented in the radial direction of the ring discharger.

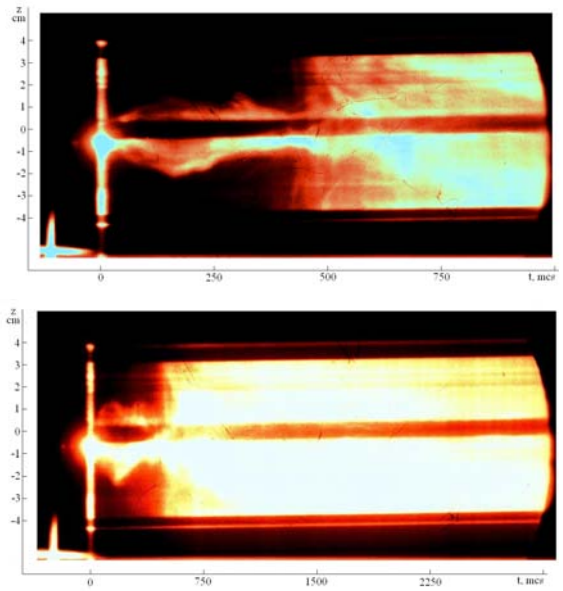

(a)

(b)

Fig. 21

Typical streak images of glow in the reactor. The slit of the streak camera is oriented along the Z axis.

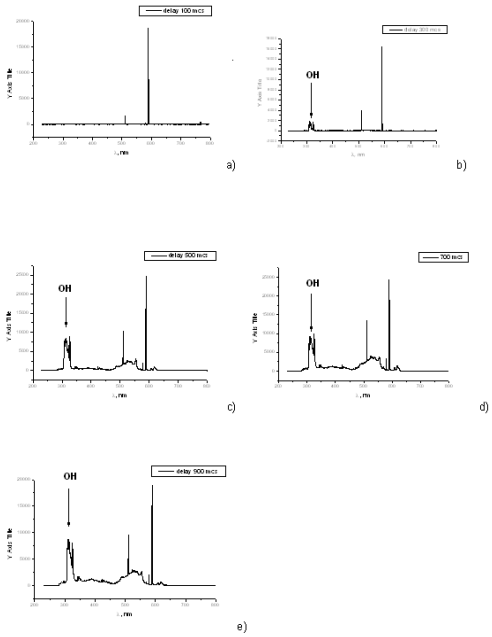

Fig. 22
Typical optical spectra of reactor radiation measured with different delay time t with respect to discharge initiation: a) t=100μs; b) t=200μs; c) t=500μs; d) t= 700μs; e) t=900μs.

Figure 23 shows typical shadow photographs taken in the direction orthogonal to the plane of the ring when operating with a methane—oxygen mixture (CH_4:O_2) and oxygen (O_2). The photographs correspond to different delay times counted from the discharger trigger pulse.

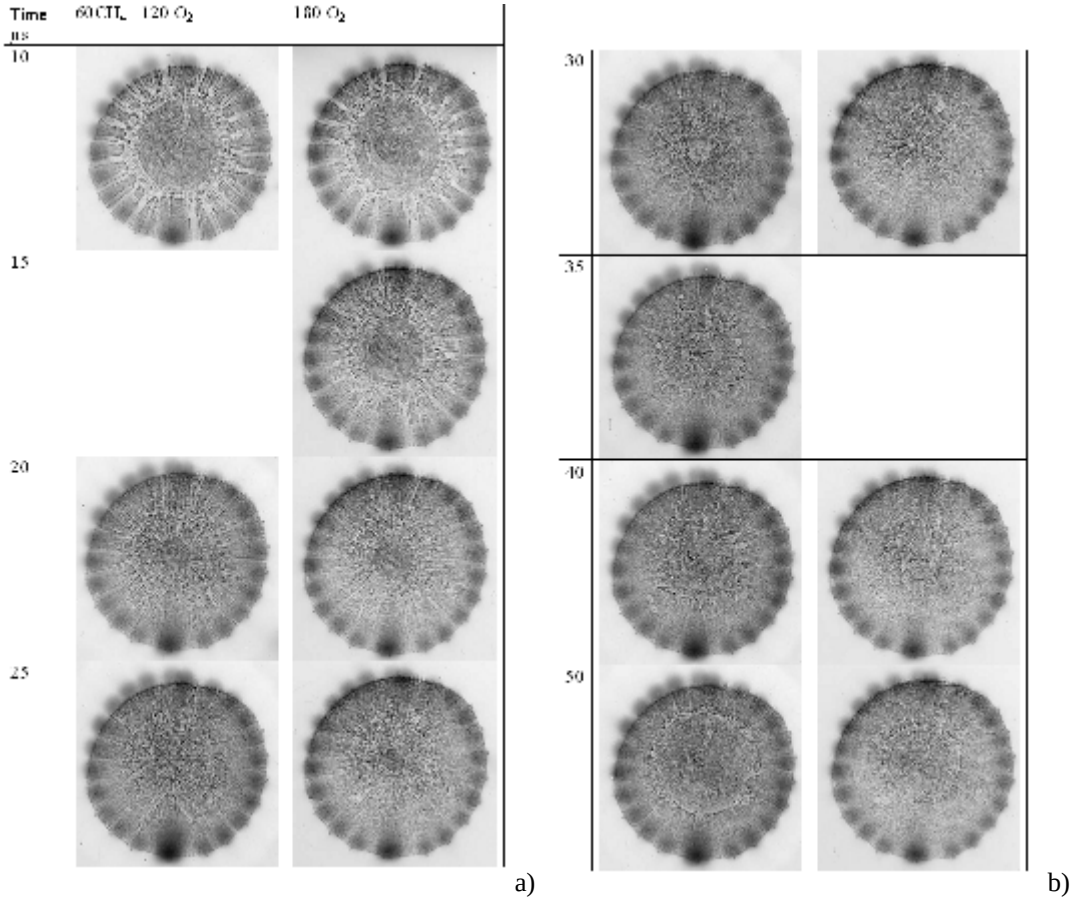
Time
60 CH4 120 O2 180 O2
ns
10
15
20
25
30
35
40
50
60
70
80
90
100
200
300
400

a) b)

c) d)

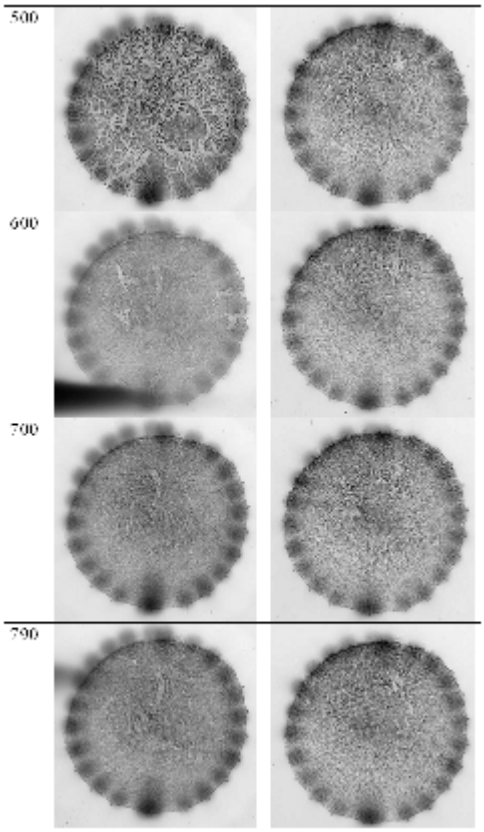

e)

Fig. 23
Shadow photographs for different delay time t counted from discharger trigger pulse. Left column for a discharge in the CH_4:O_2 mixture; right column for a discharge in O_2. Delay time t in μs is indicated near the each line.

Figures 24 and 25 show typical waveforms of the 'refraction' signals measured when operating with a noncombustible gas (180 Torr) and a methane—oxygen mixture, respectively.

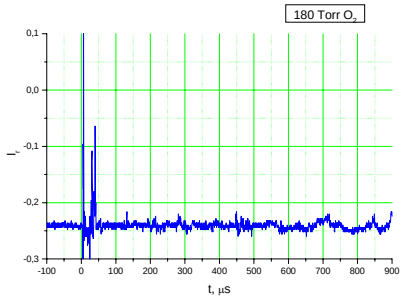

Fig. 24
Signal from the refraction detector. Discharge in O_2 .

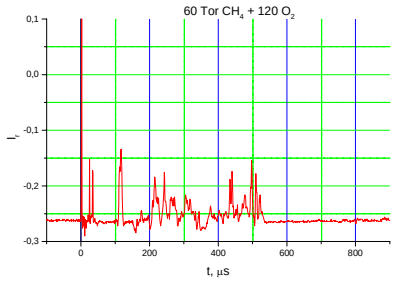

Fig. 25.
Signal from the refraction detector. Discharge in a CH_4:O_2 mixture.

In Fig. 26, a time corresponding to the maximum intensity of the radiation integrated over the spectrum (see Fig. 18) and the OH band (see Fig. 19) is plotted versus the energy released in the ring discharger.

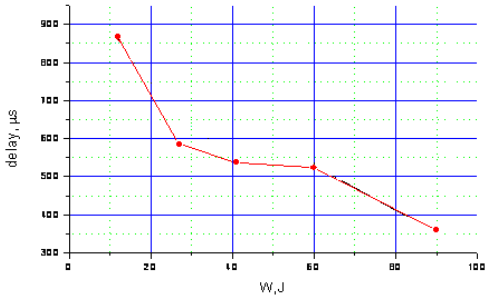

Fig. 26
Delay time for maximum OH band radiation as a function of the energy W released in the ring discharge.

Analysis of experimental results allows us to conclude that geometry of the electric-discharge initiator, namely its ring geometry, plays a decisive role in the process of ignition of a combustible gas mixture as well as in the dynamics of the propagation of a flame inside the combustion chamber.

As we might expect, the ignition of a gas mixture begins near the annular plasma layer (see Fig. 20). In this case, the flame penetrates the surrounding gas at low velocities, which do not exceed the velocity of usual deflagration waves. As a consequence, the flame initiated by the annular plasma layer is confined to this region during the time interval under observation. A peculiarity of the phenomenon under study is that an extremely fast process of flame propagation throughout the chamber volume starts in the region situated at a distance from the annular region of energy release – at the axis of the ring, near its center.

Oscillograms of photomultiplier signals and FER-7 streak images of a glow in the reactor allow us to distinguish three characteristic time intervals (phases), as illustrated by Fig. 27. Here, one can see a photomultiplier signal, a streak picture and several shadow pictures for different delay times.

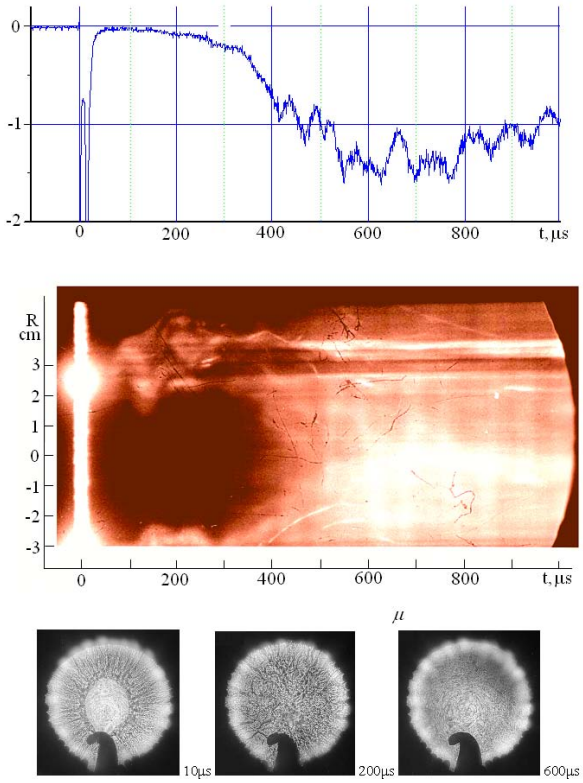

Fig. 27

The three photographic layers show, from top to bottom: a photomultiplier signal measuring the reactor radiation integrated over the spectrum; a streak image of glow in the reactor, the slit of the streak camera being oriented in the radial direction of the discharger; typical shadow pictures of gasdynamic processes in the plane of the ring during discharge in a methane-oxygen mixture.

The first phase is a very short period Δt_1 (in this case $\Delta t_1 \cong 5 - 10$ μs) during which a discharge is excited along the initiator surface and an annular plasma layer forms, and the energy is released to a gas layer adjacent to the inner surface of the discharger through gas-discharge plasma.

The second phase is associated with a feeble glow recorded in the streak picture and identified as a wave propagating from the ring to the axis (Fig. 10). The duration of this phase, in which the photomultiplier signal becomes zero (Figs. 6, 7), is $\Delta t_2 \cong 200 - 300$ μs.

The third phase is associated with a fast volume combustion of the mixture, recorded in the streak picture as a bright burst of duration $\Delta t_3 \cong$ 5-10 ms .

The presence of three phases with their characteristic features is typical of previous experiments in closed quartz tubes filled with a methane—oxygen mixtures, where the combustion was initiated by high-power linear gliding discharges, microwave discharges on plane metal—dielectric targets, laser sparks. Though seemingly identical to the sequence of events in [7-10], the initiation of combustion in the present experiments demonstrates also its distinctive features, especially, in the second phase of the process, when the combustible gas is being prepared to the fast (‘explosive’) combustion. The features peculiar to the initiation of combustion by a ring discharge show up if we consider in more detail the experimental results concerning the measurements of radiation and gas-dynamic characteristics of the methane—oxygen medium in the phase preceding the ignition.

Shadow photographs of gas-dynamic perturbations in the cross-sectional plane of the ring discharger show that the processes of formation of a ring (toroidal) shock wave, its

convergence toward the axis and reflection at the axis proceed in almost the same way in the combustible (methane—oxygen) and noncombustible (oxygen) medium (see Fig. 23a, 23b). In this initial phase ($t \leq 60$ μs), a glow is visible only in a layer of discharge plasma adjacent to the inner surface of the ring (Fig. 20), whereas neither the photomultiplier nor FER-7 detect glow inside the ring.

The optical radiation from the reactor is absent in noncombustible gases (oxygen) at a time $t > 100$ μs. At this post-discharge time in chemically inactive gases, the indications of the presence of gas-dynamic perturbations against the background are missing from the shadow photographs and the refraction detector signals (see Figs. 23c, 23d, 23e and Fig. 24). However, the absence of any consequences of the ring discharge at delay times > 100 μs is characteristic of only discharges in oxygen. An essentially different type of situation occurs in methane—oxygen mixtures. In this case, a feeble but well-defined glow appears within 50-60 μs in the streak image. This glow is identified as a wave which propagates accelerating from the surface of the ring toward its axis (Fig. 10). The average velocity of the wave is on the order of $5\ 10^4$ cm/s. Gas-dynamic processes do not cease: a radially convergent gas-dynamic wave appears in the shadow photograph; behind its front are seen local gas density perturbations, mostly in the form of extended inhomogeneities (see Figs. 23c, 23d). [Perturbations of this sort are detected by the refraction detector as well (Fig. 15)]. The average velocity of this second convergent wave is nearly equal to the velocity of the first glow wave ($\sim 5\ 10^4$ cm/s). Convergence of the second gas-dynamic wave at the axis of the ring ($t \cong 300 - 400$ μs) is accompanied by a burst of light, as is seen from the photomultipler signals (radiation integrated over the spectrum and OH band, Figs. 16, 17, 20), which indicates the volume combustion.

In the context of gas dynamics, the ignition process in oxygen may be interpreted as the following sequence of events: the excitation of a shock wave by discharge, the cummulative process of convergence of this wave toward the axis, its reflection at the axis and reverse motion from the center of the ring. At this point, the gas-dynamic response of the medium to the ring discharge ceases. Other chemically inactive gases show a similar behavior. In the methane—oxygen medium, however, the process goes in so far as the second radially convergent wave appears, and eventually its focusing at the axis is accompanied by ignition of the methane—oxygen mixture.

Flame initiated at the axis of the ring, in the vicinity of the center is accompanied by a combustion wave, which at a velocity on the order of 10^5 cm/s travels in both the axial and radial directions, and within 100 μs and even sooner, combustion occurs throughout the reactor volume. After the second wave approaches the axis, perturbations extended in the radial direction disappear in shadow photographs (Figs. 23d, 23e), where perturbations show up as spots distributed chaotically over the cross-sectional area.

Subsequently, when the intensity of radiation, associated with flame, reaches its maximum and then slowly decreases ($t \geq 600$ μs), the field of shadow photographs becomes free from local inhomogeneities represented perturbations of the medium (see Fig. 23e). At the same time, characteristic fluctuations which are due to perturbations of the medium disappear from the refraction detector signal (Fig. 25). The results obtained late in the post-discharge phase with the help of shadow photography and refraction measurements testify to the volume combustion of the mixture throughout the reactor and to equalization of the gas temperature (apparently, at a level of the equilibrium burnout temperature of a stoichiometric methane—oxygen mixture).

Of particular interest is the mechanism for formation of a feeble glow wave convergent at the axis and preceding the ignition. This wave exhibits properties similar to feeble glow waves – predecessor events, observed in our previous experiments on the ignition of methane—oxygen mixtures in closed chambers by different types of high-power electric discharge. As in the present experiment, these so-called ‘incomplete combustion waves’ propagate from localized discharges into the surrounding gas at velocities far exceeding the velocity of a usual

deflagration wave (even taking into account the gas-dynamic entrainment of a burning medium, this velocity cannot exceed 4 10^3 см/с). The nature of 'incomplete combustion waves' remains an open question. The present experiment allows us to assume that one of the factors, which play a part in the formation of this phenomenon, is a peculiar kind of 'chemical' instability related to the production of excited particles and radicals in local overheated regions behind the front of a feeble glow wave. These active particles stimulating the heating promote the ignition of the gas throughout the volume. It may well be that a feeble glow recorded in the FER-7 streak pictures is due to emission from the OH radicals.

Thus, we checked experimentally our assumption that a ring electric discharge can provide ignition of a combustible methane—oxygen medium at a distance from the region of energy release, i.e., in the axial region near the center of the ring. In real situation, however, the process turns out to be more complicated than expected. Combustion is initiated not by the first (toroidal) shock wave generated by an annular plasma layer, but by the second gas-dynamic wave emergent with some delay time with respect to the first wave. The mechanism for formation of this wave is not completely understood, and the construction of a model adequately describing the processes leading to ignition at the axis calls for further investigations.

It should be noted that, besides an opportunity of initiating combustion at a distance from the region of energy release, the ring discharger ensures very short induction times, namely, time intervals between the discharge initiation and the initiation of combustion). The induction time depends markedly on the energy released in the discharge: its value decreases with increasing energy and reaches ~ 350 μs at W ≅ 90 J (Fig. 16). Such a dependence shows that the mechanism for initiating the volume combustion by a ring discharge in a closed chamber can in no way be explained by a usual deflagration wave excited by discharge.

Finally, the work under the Project was completed by Task 7 consisting in the construction of a mathematical model of the process of cumulative convergence of a toroidal shock wave in a methane—oxygen gas mixture. For describing the flows, we used the set of gas-dynamic equations of an ideal gas medium in cylindrical coordinates:

$$\frac{\partial(\rho r)}{\partial t} + \frac{\partial(\rho u r)}{\partial z} + \frac{\partial(\rho v r)}{\partial r} = 0, \quad (6)$$

$$\frac{\partial(\rho_i r)}{\partial t} + \frac{\partial(\rho_i u r)}{\partial z} + \frac{\partial(\rho_i v r)}{\partial r} = \omega_i r, \quad (7)$$

$$\frac{\partial(\rho u r)}{\partial t} + \frac{\partial[(p + \rho u^2) r]}{\partial z} + \frac{\partial(\rho u v r)}{\partial r} = 0, \quad (8)$$

$$\frac{\partial(\rho v r)}{\partial t} + \frac{\partial(\rho u v r)}{\partial z} + \frac{\partial[(p + \rho v^2) r]}{\partial r} = p, \quad (9)$$

$$\frac{\partial[(H - p) r]}{\partial t} + \frac{\partial(H u r)}{\partial z} + \frac{\partial(H v r)}{\partial r} = 0, \quad (10)$$

$$H = \sum_{i=1}^{N} \rho_i h_i + \rho \frac{u^2 + v^2}{2} \quad (11)$$

where N=4 is the number of mixture components; ρ_i and h_i are the mass density and enthalpy of the *i*th component respectively; ω_i the rate of ρ_i variation in chemical reactions; H is the total enthalpy. The caloric and thermic equations of state for the mixture are as follows:

$$h_i = c_{0i} + c_{p_i} T \quad (12)$$

$$p = \sum_i \frac{\rho_i}{\mu_i} R_0 T \quad (13)$$

where T is the mixture temperature, μ_i is the molar mass of the *i*th component, and R_0 is the absolute gas constant.

We use a single-stage kinetics model, in which the combustion of the methane—oxygen mixture is described by only one reaction according to the stoichiometric equation

$$CH_4 + O_2 \rightarrow 2H_2O + CO_2 \quad (14)$$

In this model, we assume that the mixture consists of four components, and the reaction rate defines all ω_i according to the equalities

$$\frac{\omega_{CH_4}}{\mu_{CH_4}} = \frac{\omega_{O_2}}{2\mu_{O_2}} = -\frac{\omega_{H_2O}}{2\mu_{H_2O}} = -\frac{\omega_{CO_2}}{\mu_{CO_2}} = A T^{\beta} e^{-\frac{E}{R_0 T}} \left(\frac{\rho_{CH_4}}{\mu_{CH_4}}\right)^a \left(\frac{\rho_{O_2}}{\mu_{O_2}}\right)^b , \quad (15)$$

where subscripts *i* are replaced with the component symbols.

The gas-dynamic equations were solved numerically by using Godunov's modified explicit scheme of first order of accuracy over space and time on a fixed multiple-shell mesh, which specially separated the electric-discharge zone. The computations were performed in the domain bounded by the solid chamber walls. The boundary condition was that the flow vanishes on the walls. Energy release was modeled by an increase in the internal energy of the gas uniformly over the discharge region. Two cases have been considered: the energy is released instantaneously at the initial time or steadily during a specified time interval.
A full time-dependent picture of flows in the chamber has been recorded. Besides, we recorded the gas-dynamic parameters at the center of the discharge region, at the center of the chamber and the points (z, r) near the chamber walls. Using the above data, we performed computer animation of fields of gas-dynamic parameters in the chamber.

The calculations have shown that, in the case of instantaneous energy release, the cumulative convergence of the first toroidal wave toward the axis will be accompanied its transformation into a detonation wave only at values of released energy that far exceed (by an order of magnitude and more) the energy released in our experiments.

In the case where the energy is released within a certain time interval and its value is at a level of the energy used in our experiment (~30 J), the calculations we observed a fast inflammation of the mixture in the chamber volume. The ignition times in this case are at a level of times observed in the experiment (on the order of 400 μs). The ignition mechanism is attributed to multiple interaction between the ring shaped discharge zones and shock waves reflected from the ends and walls of the chamber. Typical pictures of gas-dynamic and thermodynamic processes for the former and latter cases are shown in Figs 28 and 29 respectively.

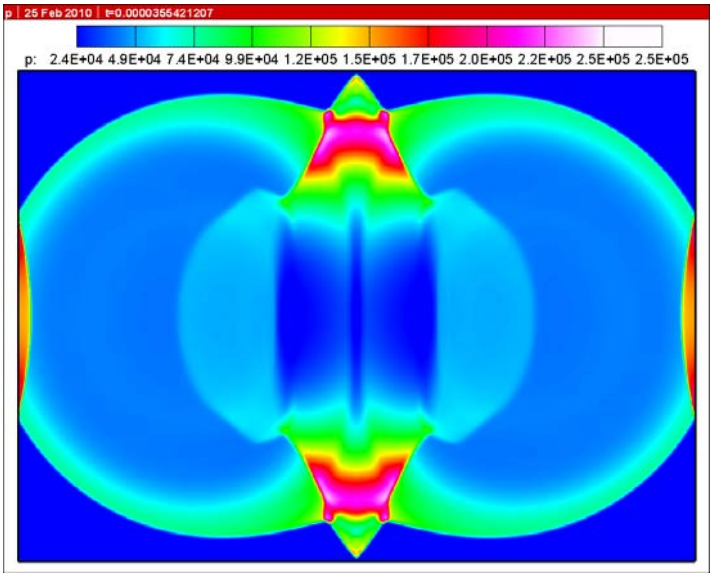

Fig. 28.
Pressure distribution in R-Z plane. t=35.5 μs.

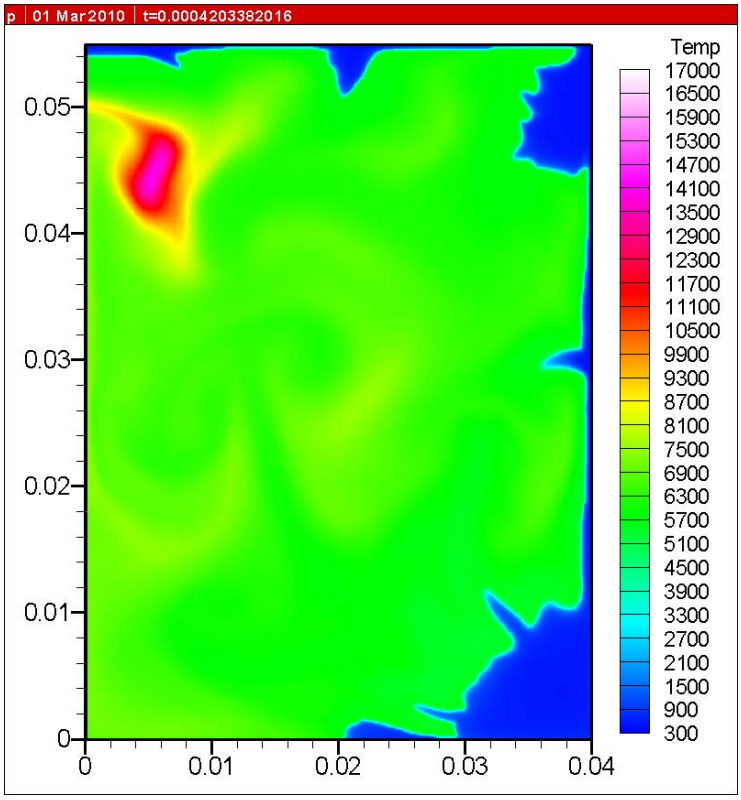

Fig. 29.
Temperature distribution in R-Z plane. t=420 μs.

Conclusions

In the course of implementation of the Project, we carried out experiments for studying the generation of a toroidal shock wave by ring electric discharge in atmospheric-pressure air. It was shown that the shock wave converges at the axis of the ring. A mathematical model describing the focusing of a non-one-dimensional shock wave was constructed, and the results of calculations were compared with the experimental results. The energy released in the ring discharge was estimated from calculations given a good fit to the experimental dynamics of a toroidal shock wave convergent toward the axis and also axial shock waves (Mach waves) accompanying the cumulative process of focusing. The theory is in good agreement with the experiment, on the assumption of instantaneous release of energy close to that used in our experiment. With the assumption that the model adequately describes actual gas flows at a given level of released energy, the gas temperature was estimated near the cumulation region on the axis at some distance from the center of the ring. In particular, for a ring discharger of radius ~5 cm with released energy of about 200 J, the gas temperature on the axis of the ring at a distance of about 1 cm from its center was estimated as 6000 K.

At the second stage of the work under the Project, the aim of studies was the experimental demonstration of distant heating and ignition of a methane—oxygen stoichiometric mixture with the help of a multielectrode discharger generating an annular plasma layer giving rise to strong gas-dynamic perturbations converging radially toward the axis.

Gas-dynamic consequences of ring discharge in the methane—oxygen medium differ from the consequences of discharges in chemically inactive gases and are more complicated. In this case, the second radially convergent wave of strong gas-dynamic perturbation arises. Behind the front of the second shock wave, we observe a radial flow of the strongly perturbed (with respect to density and temperature) gas with small-scale inhomogeneities extended in the radial direction from the ring discharge toward the axis. The moment of inflammation near the axis is close to the moment at which these inhomogeneities approach the axis. Combustion initiated near the axis propagates throughout the chamber volume at velocities far exceeding the velocities of usual deflagration waves.

The induction times provided by the ring discharge turn out to be much shorter than the induction times typical of experiments in which combustion is initiated by linear gliding surface discharges, microwaves discharges at plane targets and laser spark discharges of the same or nearly the same energy.

Thus, analyzing experimental results, we can conclude that the geometry of the electric-discharge initiator, i.e., its ring-shaped structure, plays a decisive role in the process of ignition of a combustible gas mixture, as well as in the dynamics of flame propagation through the volume of the combustion chamber.

The theoretical (mathematical) model has been constructed for describing gasdynamic and thermodynamic processes occurring when annular discharge is excited in a closed chamber filled with a methane--oxygen mixture. The calculated ignition times turn out to be close to the induction times measured experimentally. It is shown that the ignition mechanism is related to multiple interactions with ring-shaped discharge zones of shock waves reflected from the ends and walls of the chamber.

Attachment 1: List of published papers and reports

[1] S.Yu.Kazantsev, I.G.Kononov, I.A.Kossyi, N.M.Tarasova and K.N.Firsov. Ignition of a Combustible Gas Mixture by a Laser Spark Excited in the Reactor Volume // Plasma Physics Reports, v. 35, No 5, 2009, pp. 251-257.

The process of initiation of combustion of a stoichiometric CH_4:O_2 mixture in a closed chamber by laser spark excited far from the walls is studied experimentally. It is shown that the laser spark is accompanied by an "incomplete combustion wave" detected by a low-intensity radiation in the optical spectral range. The velocity of this wave far exceeds the velocity of the combustion wave and is much lower than the velocity of the detonation wave.

Within delay times of 500–700 μs, a bright burst throughout the chamber volume indicates the rapid (based on branching chain reactions) ignition of the gas mixture.

The conclusion is made concerning a common nature of the processes of the initiation of combustion in combustible gas mixtures by laser sparks excited far from the walls and the processes of previously investigated initiation by laser sparks at solid targets, high-power microwave discharges, and high-power slipping surface discharges.

[2] N.K.Berezhetskaya, S.I.Gritsinin, V.A.Kop’ev, I.A.Kossyi, P.S.Kuleshov, N.A.Popov, A.M.Starik and N.M.Tarasova. Initiation of Combustion in an Enclosed Volume by High-Power Electric Discharge // Plasma Physics Reports, v. 35, No 6, 2009, pp. 471-483..

Results are presented from experimental studies and numerical simulation of the process of initiation of combustion of a stoichiometric gas mixture CH_4--O_2 by high-current gliding surface discharge, It is shown that such a discharge generates an axially propagating

heat wave (predecessor wave). When traveling in the gas, this wave promotes the heating of the gas volume and is followed by nearly simultaneous ignition of the gas mixture throughout the reactor volume.

[3] E.M.Barkhudarov, T.S.Zhuravskaya, I.A.Kossyi, V.A.Levin, V.V.Markov, N.A.Popov, N.M.Tarasova, S.M.Temchin and M.I.Taktakishvili. Axissymmetric Electric Discharge as a Method for Gas Heating at a Distance // Plasma Physics Reports, v. 35, No.11, 2009, pp. 924-932.

Experimental and theoretical studies have been made of gas-dynamic phenomena accompanying the excitation of annular electric discharge in air at atmospheric pressure. It is shown in experiment that the discharge generates a toroidal (three-dimensional) shock wave that converges at the axis thus producing a cumulative effect. A mathematical model has been constructed for describing the process of focusing of a toroidal shock wave. The results of measurements of shock processes accompanying the discharge agree well with the results of simulation. For this reason, it is possible to estimate the gas temperature value that can be attained in the region of convergence at some distance from the ring center.

[4] E.M.Barkhudarov, T.S.Zhuravskaya, I.A.Kossyi, V.A.Levin, V.V.Markov, N.A.Popov, M.I.Taktakishvili and S.M.Temchin. Convergent Toroidal Shock Wave as a Possible Igniter of Combustible Gas Mixture Flow on its Axis // 47th AIAA Aerospace Sciences Meeting and Exhibition, 5-8 January, 2009, Orlando, Florida, Report AIAA 2009-1555.

Experimental and theoretical studies of gas-dynamic phenomena accompanying electric discharges excited in air at atmospheric pressure are reported on. It is shown in experiment that the discharge generates a toroidal (three-dimensional) shock wave that converges at the axis thus producing a cumulative effect. A mathematical model has been constructed for describing the process of focusing of a toroidal shock wave. The results of measurements of shock processes accompanying the discharge agree well with the results of calculations. This makes it possible to estimate the gas temperature value that can be attained in the region of convergence at some distance from the ring center. The ring electric discharge is examined as a possibility for initiation of combustion in fuel-air flows in their axial region.

[5] N.K.Berezhetskaya, S.I.Gritsinin, A.M.Davydov, I.A.Kossyi, V.A.Kop'ev, N.M.Tarasova. Gas Discharges with High Specific Energy Release Like Igniters of Closed Volumes or Fluxes of Combustible Gases // ISPC 19, Book of Abstracts, Ruhr-University Bochum, Germany, 2009, Ed. by A. Von Kendell, J.Winter, M.Boke, V.Schulz-von der Gathen, p. 619.

The main purpose of the work is to study the initiation of combustion of gas mixtures by electric discharges with high specific energy released in the discharge volume. The discharges of this kind are sources of intense UV radiation penetrating the surrounding gas and have a peculiar geometry (which is rater complicated in number of cases).

[6] E.M.Barkhudarov, T.S.Zhuravskaya, I.A.Kossyi, V.A.Levin, V.V.Markov, N.A.Popov, N.M.Tarasova, S.M.Temchin and M.I.Taktakishvili. Created by Annular Electric Discharge Nonplanar Shock Wave as a Mean of Distant Heating and Ignition of Flammable Gas // in

"Nonequilibrium Phenomena. Plasma, Combustion, Atmosphere" (NEPCAP 2009), Ed. by G.D.Roy, S.M.Frolov, A.M.Starik, Torus Press, Moscow, 2009, pp. 138-141.

The paper describes results of experiments for studying the cumulative process of convergence of a toroidal shock wave, generated by a ring electric discharge and converging toward the axis, in atmospheric-pressure air. A mathematical model is described that was used in numerical simulation of the process of convergence of a toroidal shock wave.

A comparison is made of the results of simulation and experiments in order to estimate the temperature that may be achieved near the axis (in the region of energy cumulation). It is shown that this temperature can reach 6000 K under the experimental conditions.

[7] S.Yu.Kazantsev, I.G.Kononov, I.A.Kossyi, N.M.Tarasova and K.N.Firsov. Ignition of Flammable Gas Mixture in a Closed Volume by Direct CO_2-Laser Heating of Gas Layer // in "Nonequilibrium Phenomena: Plasma, Combustion, Atmosphere", (NEPCAP 2009), Edited by G.D.Roy, S.M.Frolov, A.M.Starik, Torus Press, Moscow, 2009, p. 207.

The paper presents results of investigations of the initiation of combustion of a stoichiometric CH_4:O_2:SF_6 mixture by means of direct local heating of the gas by a pulsed beam of a high-power CO_2-laser.

It is shown that the deflagration wave transforms into a detonation wave at very small distances from the region of the mixture ignition.

[8] S.Yu.Kazantsev, I.G.Kononov, I.A.Kossyi, N.M.Tarasova and K.N.Firsov. Ignition of Gaseous Methane-Oxygen Mixture in Closed Volume by a Freely Localized Spark Generated by HF Laser // in "Nonequilibrium Phenomena: Plasma, Combustion, Atmosphere", (NEPCAP 2009), Edited by G.D.Roy, S.M.Frolov, A.M.Starik, Torus Press, Moscow, 2009, pp. 208-209.

The paper presents results of the experiment on the initiation of combustion of a methane-oxygen mixture by laser spark inside the chamber.

Conclusions have been drawn about a common nature of the initiation of combustion by laser spark and by previously investigated methods of the initiation of combustion by laser spark at a solid surface, by microwave discharge and high-current gliding surface discharge.

[9] Firsov K.N., Kazantsev S.Yu., Kononov I.G., Kossyi I.A., Tarasova N.M. Ignition of methane-oxygen gas mixture in closed volume by freely localized laser spark and pulse laser heating of the gas // VI Int. Conference "Plasma Physics and Plasma Technology", Contributed Papers, v. I, pp. 130-133, Minsk, Belarus, 2009, B.I.Stepanov Inst. Of Physics, National Academy of Sciences of Belarus.

The paper presents results of the experiment on the initiation of combustion of a methane-oxygen mixture by laser spark inside the chamber.

Conclusions have been drawn about a common nature of the initiation of combustion by laser spark and by previously investigated methods of the initiation of combustion by laser spark at a solid surface, by microwave discharge and high-current gliding surface discharge.

Results are presented from studies of ignition of a stoichiometric CH_4:O_2:SF_6 mixture by means of direct local heating of the gas by the pulsed beam of a high-power CO_2-laser.

[10] I.A.Kossyi, E.M.Barkhudarov, T.S.Zhuravskaya, V.A.Levin, V.V.Markov, N.A.Popov, M.I.Taktakishvili and WS.M.Temchin. Axisymmetric Electric Discharge as a Method for Gas

Heating Distance // The 8th International Workshop on Magneto-Plasma Aerodynamics, Abstracts, pp. 88-89, 2009, Moscow.

Gas-dynamic phenomena accompanying a ring electric discharge excited in atmospheric-pressure air have been studied experimentally and theoretically. It is shown experimentally that the discharge generates a toroidal (three-dimensional) shock wave that converges toward the axis. A mathematical model describing the focusing of a toroidal shock wave is constructed. The measured characteristics of shock processes accompanying the discharge agree well with results of calculations. This makes it possible to estimate the temperature that can be achieved in the shock wave at a certain distance from the ring discharge.

[11] N.K.Berezhetskaya, S.I.Gritsinin, A.M.Davydov, S.Yu.Kazantsev, I.G.Kononov, I.A.Kossyi, P.S.Kuleshov, N.A.Popov, A.M.Starik, N.M.Tarasova, K.N.Firsov. Gas Discharges with High Specific Energy Release Like Igniters of Closed Volumes or Fluxes of Combustible Gases // The 8th International Workshop on Magneto-Plasma Aerodynamics, Abstracts, pp. 13-15, 2009, Moscow.

The paper presents results of experimental studies and numerical simulation of the process of ignition of a stoichometric gas mixture CH_4-O_2 by high-current gliding surface discharge. It is shown that the discharge gives rise to a heat wave (predecessor wave) that propagates in the direction along the z-axis, penetrates the gas medium and promotes a fast gas heating and, then, an almost simultaneous ignition of the gas throughout the reactor.